Growth Induced Reordering of Fullerene Clusters Trapped in a Two-Dimensional Supramolecular Network

J. A. Theobald,[†] N. S. Oxtoby,[‡] N. R. Champness,[‡] P. H. Beton,*[,†] and T. J. S. Dennis[§]

Schools of Physics & Astronomy and Chemistry, University of Nottingham, Nottingham NG7 2RD, United Kingdom, and Department of Chemistry, Queen Mary, University of London, Mile End Road, London E1 4NS, United Kingdom

Received October 6, 2004. In Final Form: December 21, 2004

We have investigated the growth of molecular clusters in confined geometries defined by a bimolecular supramolecular network. This framework provides a regular array of identical nanoscale traps in which further deposited molecules nucleate cluster growth. For the higher fullerene, C_{84}, molecules aggregate into close packed assemblies with an orientation which switches when the cluster size increases by one molecule. This change is controlled by the interactions between the molecules and the confining boundaries of the network pore. We show that, following nucleation of small clusters, further growth requires a reconfiguration of previously captured molecules resulting in a transition between nanoscale phases with different ordering.

Recent advances in two-dimensional self-assembly have led to a new type of nanostructured surface on which arrays of nanoscale pores may be formed. These pores have been shown to act as traps for adsorbed molecules resulting in novel growth processes which have been demonstrated using both organic and inorganic networks.[1−3] The arrays provide a means of controllably introducing a network of "artificial" step edges onto a surface. The presence of steps plays a key role in the nucleation and growth of monolayer and multilayer thin films on conventional substrates,[4] and the self-assembled networks offer a greatly enhanced control of the available geometry and density of the steps. In particular, the effective step density available for self-assembled nanoporous surfaces may be much higher and the dimensionality can be different; in particular closed two-dimensional loops enclosing nanoscale areas with dimensions 1−3 nm may be readily formed.[1−3] The arrays provide an ideal experimental framework for the study of growth within a nanoscale confined geometry.

In this paper we discuss the capture, nucleation, and growth of molecular clusters within bounded nanoscale areas, or pores, on a nanostructured surface formed by a supramolecular network. In particular, we observe a set of population dependent molecular clusters with different directional order. The stability of these structures is determined by the interplay between intermolecular and molecule−network interactions, and our results show that the artificial edges control not only the nucleation but also the stabilization of the population dependent nanophase.

The nanostructured surface used in this study is a self-assembled bimolecular network, which is stabilized by hydrogen bonding. Spontaneous ordering of molecular networks using noncovalent intermolecular interactions has been studied by a number of groups over recent years.[5−12] The assembly used in this study is formed on a Ag/Si(111)-$\sqrt{3} \times \sqrt{3}$R30° surface which is prepared under ultrahigh vacuum (UHV) conditions (base pressure, 10^{-10} Torr) using established procedures.[13−15] A 7 mm × 3 mm piece of a p-doped Si(111) wafer is loaded into the UHV system, outgassed overnight at 700 °C, and then flash annealed at 1200 °C for 1 min to form the 7 × 7 reconstruction. Ag was then sublimed onto the Si(111)-7 × 7 surface at a rate of 0.3 nm/min while the Si substrate was annealed at 550 °C in order to form the Ag/Si(111)-$\sqrt{3} \times \sqrt{3}$R30° reconstruction. The supramolecular network is formed by first subliming 0.3 monolayers (ML) of perylene tetracarboxylic diimide (PTCDI) onto the Ag/Si(111)-$\sqrt{3} \times \sqrt{3}$R30° surface which is held at room temperature. This is followed by the sublimation of melamine (1,3,5-triazine-2,4,6 triamine) while annealing the substrate at a temperature of 100 °C. The structure of these molecules and a schematic showing their interaction via hydrogen bonding are shown in Figure 1a−c. Due to their symmetry and commensurability with the Ag/Si(111)-$\sqrt{3} \times \sqrt{3}$R30° surface, the molecules assemble into a hydrogen bonded honeycomb network in which melamine and PTCDI respectively form the vertexes and edges of the hexagonal repeat unit (see Figure 1c).[1] Images of the surface are acquired using a scanning tunneling

[†] School of Physics & Astronomy, University of Nottingham.
[‡] School of Chemistry, University of Nottingham
[§] Department of Chemistry, Queen Mary, University of London.

(1) Theobald, J. A.; Oxtoby, N. S.; Phillips, M. A.; Champness, N. R.; Beton, P. H. *Nature* **2003**, *424*, 1029.
(2) Corso, M.; Auwarter, W.; Muntwiler, M.; Tamai, A.; Greber, T.; Osterwalder, J. *Science* **2004**, *303*, 217.
(3) Stepanow, S.; Lingenfelder, M.; Dmitriev, A.; Spillmann, H.; Delvigne, E.; Lin, N.; Deng, X. B.; Cai, C. Z.; Barth, J. V.; Kern, K. *Nat. Mater.* **2004**, *3*, 229.
(4) Brune, H. *Surf. Sci. Rep.* **1998**, *31*, 121.
(5) Chen, Q.; Richardson, N. V. *Nat. Mater.* **2003**, *2*, 324.
(6) De Feyter, S.; De Schryver, F. C. *Chem. Soc. Rev.* **2003**, *32*, 139.
(7) Barth, J. V.; Weckesser, J.; Cai, C.; Gunter, P.; Burgi, L.; Jeandupeux, O.; Kern, K. *Angew. Chem., Int. Ed.* **2000**, *39*, 1230.
(8) Bohringer, M.; Morgenstern, K.; Schneider, W. D.; Berndt, R. *Angew. Chem., Int. Ed.* **1999**, *38*, 821.
(9) Furukawa, M.; Tanaka, H.; Kawai, T. *Surf. Sci.* **2000**, *445*, 1.
(10) Griessl, S.; Lackinger, M.; Edelwirth, M.; Hietschold, M.; Heckl, W. M. *Single Mol.* **2002**, *3*, 25.
(11) Keeling, D. L.; Oxtoby, N. S.; Wilson, C.; Humphry, M. J.; Champness, N. R.; Beton, P. H. *Nano Lett.* **2003**, *3*, 9.
(12) Yokoyama, T.; Yokoyama, S.; Kamikado, T.; Okuno, Y.; Mashiko, S. *Nature* **2001**, *413*, 619.
(13) Upward, M. D.; Moriarty, P.; Beton, P. H. *Phys. Rev. B* **1997**, *56*, R1704.
(14) Wan, K. J.; Lin, X. F.; Nogami, J. *Phys. Rev. B* **1993**, *47*, 13700.
(15) Takahashi, T.; Nakatani, S.; Okamoto, N.; Ichikawa, T.; Kikuta, S. *Surf. Sci.* **1991**, *242*, 54.

10.1021/la047533w CCC: $30.25
Published on Web 02/04/2005

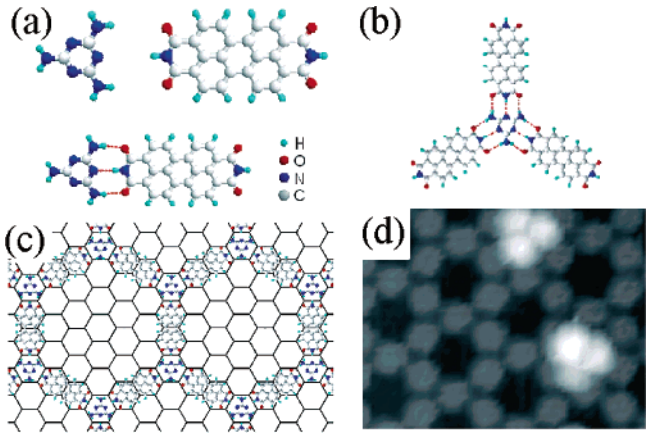

Figure 1. (a) Molecular structure of PTCDI, melamine, and their interaction through hydrogen bonds which are represented by dotted lines. (b) Threefold PTCDI−melamine junction stabilized by hydrogen bonds. (c) Schematic showing the molecular configuration of the self-assembled melamine−PTCDI network. The background honeycomb configuration represents the underlying Ag/Si(111)-$\sqrt{3} \times \sqrt{3}$R30° surface; Si and Ag trimers are placed respectively at the vertexes and centers of the hexagons in accordance with the accepted model for this reconstruction (ref 15). (d) STM image (12 nm × 10 nm) of C_{84} on the melamine−PTCDI network showing a low fraction of pores occupied by molecular clusters.

microscope (STM) housed within the UHV system and operating in constant current mode at room temperature.

We have previously investigated[1] the adsorption of C_{60} onto this network and have found that ordered clusters are captured within the network pores. In the present paper we extend this study to an investigation of the higher fullerene, C_{84}. This molecule was chosen since it is ~10% larger than C_{60} and the steric packing and growth within the nanoscale pores of the network are therefore expected to show significant differences. C_{84} was prepared by arc burning of graphite rods in a He stream followed by isolation and purification (including removal of minor isomers) using high performance liquid chromatography (HPLC).[16,17] The charge, consisting of approximately 1 mg of the purified D_2 isomer, was loaded into UHV and was sublimed at 455 °C at a typical rate of 0.1 ML/h.

Figure 1d shows an STM image in which the PTCDI/melamine network is resolved as the intermediate contrast honeycomb arrangement (compare with Figure 1c) and a small fraction of pores are occupied by clusters of C_{84}. For the lowest coverages of C_{84} investigated (0.05 ML), clusters of 2−7 molecules are formed in ~10% of pores, while the remainder are unoccupied indicating that C_{84} may diffuse readily across the network.

An STM image of the surface following the deposition of 0.5 ML of C_{84} is shown in Figure 2. For these higher coverages we observe clusters with 2−7 molecules. In addition, for clusters with a given number of molecules we observe several nonequivalent structures. It is immediately apparent from Figure 2 that although nearly all clusters are close packed, their orientation is size dependent. For example the principal axes of the close packing exhibited by the most common cluster, a trimer,

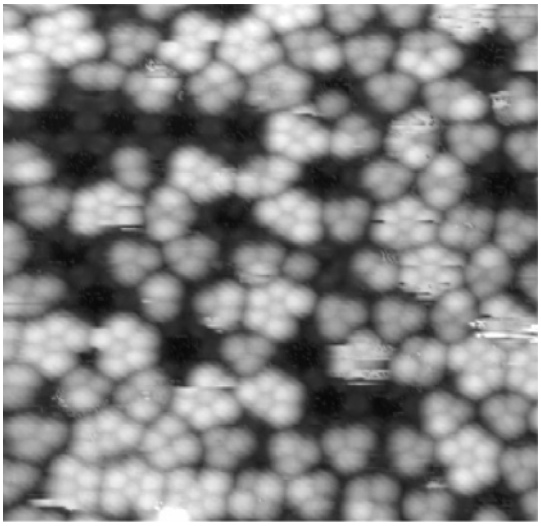

Figure 2. STM image (29 nm × 28 nm) of C_{84} clusters adsorbed on the supramolecular PTCDI−melamine network. Clusters with 2−7 molecules may be clearly resolved in this image.

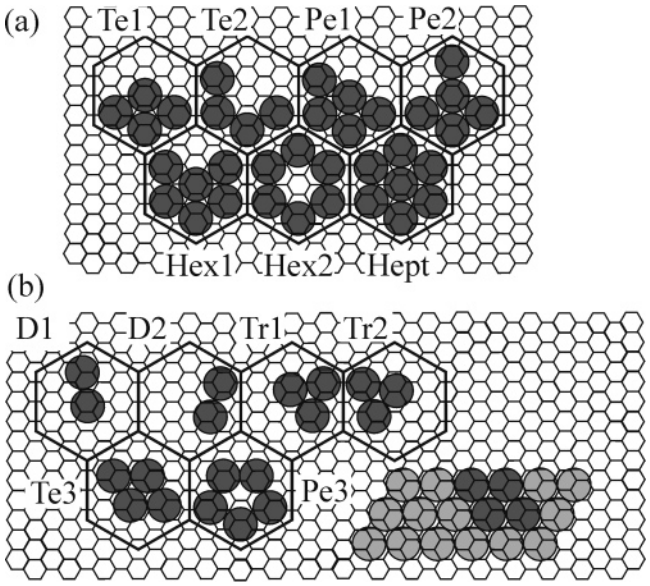

Figure 3. Schematic diagram of the placement of molecules within clusters trapped by the supramolecular network. (a) Heptamers and sub-heptamers which are close packed with a common orientational order. (b) Clusters with ordering which is different to that of the heptamers (see panel a). Also shown is the extended surface phase observed for C_{84}; the tetramer fragment of this phase is highlighted.

are misaligned with those of the hexamers and heptamers. This implies that a reordering transition must occur during growth, and we therefore classify clusters with distinct order as different nanophases which are stabilized in the confined geometry of the nanoscale pore.

The cluster configurations are shown schematically in Figure 3 in which C_{84} (diameter 1.15 nm) is drawn to scale with the underlying Ag/Si(111)-$\sqrt{3} \times \sqrt{3}$R30° surface (lattice constant, 0.665 nm) and the supramolecular network (lattice constant, 3.46 nm). The relative frequency of observation of the clusters, which is coverage dependent, is shown for this coverage in Table 1.

Figure 3a shows a set of close packed clusters which have a common orientation. These are heptamers and partially formed heptamers (sub-heptamers). For example the hexamer *Hex1* (see Figure 3) corresponds to a heptamer with one of the six outer molecules missing. A small

(16) Dennis, T. J. S.; Kai, T.; Tomiyama, T.; Shinohara, H.; Kobayashi, Y.; Ishiwatari, H.; Miyake, Y.; Kikuchi, K.; Achiba, Y. *J. Phys. Chem, A* **1999**, *103*, 8747.

(17) Dennis, T. J. S.; Margadonna, S.; Prassides, K.; Hulman, M.; Kuzmany, H. *Proceedings of the XIII International Winterschool on Electronic Properties of Novel Materials, Kirchberg, Austria, 1999*; American Institute of Physics: Melville, NY, 1999; p 187.

(18) Butcher, M. J.; Nolan, J. W.; Hunt, M. R. C.; Beton, P. H.; Dunsch, L.; Kuran, P.; Georgi, P.; Dennis, T. J. S. *Phys. Rev.* **2001**, *B64*, 195401.

Table 1. Percentage Occupation of Network Pores by the Clusters Described in Figure 3[a]

cluster	% occupation	cluster	% occupation
dimer *D1*	1.0	pentamer *Pe1*	5.0
dimer *D2*	2.5	pentamer *Pe2*	<0.5
trimers *Tr1* and *Tr2*	39.0	pentamer *Pe3*	2.0
tetramer *Te1*	2.0	hexamer *Hex1*	15.0
tetramer *Te2*	0.5	hexamer *Hex2*	0.5
tetramer *Te3*	12.0	heptamer *Hept*	3.0

[a] Analysis based on >450 pores. Clusters related by a simple symmetry operation (e.g. *Tr1* and *Tr2*) are grouped together.

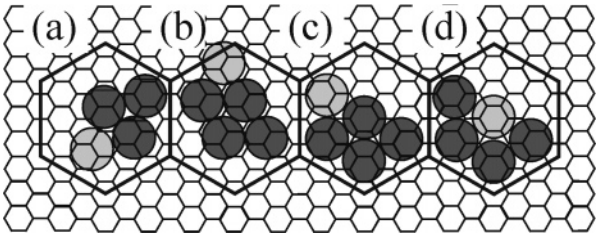

Figure 4. Capture of an additional molecule by clusters *Tr1*, *Te3*, *Te1*, and *Te2* (panels a–d, respectively). The captured molecule is shown in lighter grayscale.

proportion, ~3%, of hexamers have the central molecule missing (*Hex2*). Similarly the majority of pentamers are equivalent to heptamers with two missing molecules, most commonly two adjacent outer molecules (*Pe1*). We also observe pentamers with a pentagonal arrangement, see the top right corner of Figure 2 and further discussion below. In previous studies of the adsorption of C_{60} on this surface, heptamer and hexamer clusters were observed with a molecular spacing commensurate with the Ag/Si(111)-$\sqrt{3} \times \sqrt{3}$R30° lattice. Since C_{84} is ~10% larger than C_{60}, commensurability effects are absent and the stabilization of C_{84} clusters confirms molecular trapping is a generic property of the PTCDI/melamine network.

In Figure 3b clusters are shown which have a variety of different orientations, all of which are distinct to those of the heptamers and sub-heptamers. The most common tetramers (*Te3*), in which molecules are close packed in a rhombus, are arranged in a highly symmetric configuration with their centers coincident with the pore center and the rhombic axis parallel to a high symmetry direction of the network. Interestingly the *Te3* tetramer nanophase is equivalent to a nanoscale fragment of the extended surface phase of C_{84}.[17] This phase is shown schematically in Figure 3b with the molecules corresponding to *Te3* highlighted. Only for this cluster do molecules exhibit order equivalent to the known minimum energy surface phase.

The positions of molecules within dimers and trimers are known with a precision limited to ±0.2 nm due to tip convolution effects. Unlike the tetramers the trimers are positioned off-center with one molecule close to a vertex of the network and their edge oriented at an angle θ to the closest edge of the supramolecular network. The average measured value of θ is 19° ± 2°. Thus there are 2 inequivalent trimers (see Figure 3) which may be placed at any of the 6 vertexes of the hexagon giving 12 inequivalent configurations in total. The orientation of the trimers *Tr1* and *Tr2* does not match that of any previously observed surface phase of C_{84} or that of the heptamers and sub-heptamers. Similarly the measured molecular configuration of the dimers does not correspond to any extended surface phase of higher fullerenes. However, the measured angle between the molecules in *D2* and the adjacent network edge is 19° ± 2° matching the value of θ discussed above. Accordingly we consider *D2* to be equivalent to *Tr1* with one molecule removed. Note that the nonobservation of a trimer which is equivalent to *Te3* with one molecule removed implies that the placement of trimer molecules at unfavorable adsorption sites is compensated by molecule–network interactions. However the additional energy cost of placing a fourth molecule at an unfavorable site is not compensated.

As for the trimers and dimers, the packing orientation of the heptamers and sub-heptamers (Figure 3a) does not match any extended surface ordering showing that this phase exists only when stabilized by the supramolecular network. This indicates that molecules in these clusters sit on energetically less favorable adsorption sites and are stabilized by fullerene–network interactions.

The observation of this population dependent ordering indicates that the growth of clusters through the capture of an additional molecule is complex. In particular for the smaller clusters, for example the trimer, the capture of an additional molecule to form a tetramer requires the reordering of molecules previously incorporated in the cluster. Reordering is also required for the transitions from the dimer *D1* to a trimer, for the most common tetramer, *Te3*, to a pentamer, and for the pentagonal pentamer to a hexamer.

Growth through capture of an additional molecule is illustrated schematically in Figure 4. For a trimer (Figure 4a) a site is available for which the captured molecule simply extends the close packed cluster arrangement. However, the resulting tetramer is not observed experimentally and is therefore either energetically or kinetically unstable and transforms into one of the three tetramer configurations identified in Figure 3. Consider now the addition of a further molecule to form a pentamer. The highly symmetric tetramer does not have a close packed binding site available for a fifth molecule (see Figure 4b). In contrast a fifth molecule may be readily added to the other two tetrameric clusters as shown in Figure 4c,d, indicating that tetramers of type *Te1* and *Te2* may be more readily converted to pentamers. We note that >90% of the tetramers observed in images such as Figure 2 are of type *Te3* and argue that this abundance is due to a combination of greater energetic stability and the lack of capture sites for additional molecules.

Finally we stress the remarkable observation of the pentagonal cluster *Pe3*. The stabilization of this nonhexagonally close packed arrangement highlights the competing nature of the molecule–molecule, molecule–substrate, and molecule–network interactions. Notably the two molecules which are positioned closest to the pore center have only two nearest neighbors and, since they are not directly adjacent to a network edge, they are not stabilized by molecules within the supramolecular array. Nevertheless this arrangement is stable against relaxation to a close packed arrangement such as *Pe1* indicating that there must be a significant energy barrier to moving the central two molecules from these particular adsorption sites. The formation of this rather counter-intuitive cluster may be related to a favorable relaxation path for the *Te3* cluster on adsorbing an additional molecule, i.e., the cluster shown in Figure 4b. The smaller amount of molecular rearrangement required for the transition to the pentagonal *Pe3* rather than the hexagonal *Pe1* may result in a lower energy barrier for the transition to *Pe3*.

In conclusion we have shown that the interplay between molecule–substrate and molecule–network interactions which control the configurations of molecular clusters

nucleated in the pores of a supramolecular network leads to the stabilization of a range of nanophases. The sequential addition of single molecules leads to reordering transitions between these different clusters and demonstrates that growth within a nanoscale geometry results in new molecular structures.

Acknowledgment. We are grateful for financial support from the U.K. Engineering and Physical Sciences Council (Grant GR/S97521/01) and the European Union (Contract HPRN-CT-2002-00320).

LA047533W